

Synthesis and Electrochemical Properties of Tetranuclear Di-μ-oxo-bis[di-μ-phenolatodiiron(III)] Complexes

Yuji Miyazato,*[1,†] Masaaki Ohba,[1,††] Hiroshi Sakiyama,[2] and Hisashi Ōkawa*[1]

[1]Department of Chemistry, Faculty of Science, Kyushu University, 6-10-1 Hakozaki, Higashi-ku, Fukuoka 812-8581

[2]Department of Material and Biological Chemistry, Faculty of Science, Yamagata University, Kojirokawa, Yamagata 990-8560

Received September 14, 2006; E-mail: yujiscc@rs.kagu.tus.ac.jp

A series of tetrairon(III) complexes of di-μ-oxo-bis[di-μ-phenolatodiiron(III)] core, $[\{Fe_2(L)(L')\}_2(\mu\text{-}O)_2](PF_6)_2$ (**1**–**11**), where L^{2-} is the phenol-based macrocyclic compartmental ligand and $(L')^-$ is acetate, monochloroacetate, dichloroacetate, trifluoroacetate, pentafluoropropionate, benzoate, *p*-nitrobenzoate, pentafluorobenzoate, diethyl phosphate, diphenyl phosphate, or diethyldithiophosphate for **1**–**11**, respectively, were synthesized. X-ray crystallographic studies for **4**, **7**, and **9** indicated that two $\{Fe_2(L)(L')\}$ units were connected by two oxo bridges to afford a tetranuclear di-μ-oxo-bis[di-μ-phenolatodiiron(III)] core. Cyclic voltammograms of **1**–**11** in acetonitrile showed a quasi-reversible or irreversible reduction wave between -332 and -620 mV (vs. Ag/Ag^+), which were attributed to a two-electron process involving the $Fe_4^{III,III,III,III}/Fe_4^{II,II,III,III}$. The $Fe_4^{III,III,III,III}/Fe_4^{II,II,III,III}$ potential shifted positive with a decrease in the electron-donating ability of the end-cap ligand, and a good linear correlation was found between the potentials and the pK_a values of HL′. The $Fe_4^{II,II,III,III}$ species were generated in acetonitrile by electrochemical reduction and showed broad intervalence transition bands in the range of 900–1500 nm.

Considerable studies on tetranuclear iron complexes have been reported, because of the great interest in their magnetochemical properties or biological functions.[1–5] Alkoxide-bridged tetrairon(III) clusters, $[Fe_4(OMe)_6(dpm)_6]$ ($dpm^- = 2,2,6,6$-tetramethylheptane-3,5-dionate)[2] and $[Fe_4(OMe)_4(sae)_4]$ (sae^{2-} = 2-salicylideneamino-1-ethanol),[3] behave as single-molecule magnets. Tetranuclear iron–sulfur clusters of a cubane-type Fe_4S_4 core exist at the active site of ferredoxins, which play an essential role in electron transfer in biological systems through the $Fe_4^{II,III,III,III}/Fe_4^{II,II,II,III}$ cycle.[4,5] Electronic structure of such mixed-valence states is of particular interest in the field of inorganic chemistry apart from the biological function. Many interesting properties for polynuclear iron complexes originate from the magnetic interaction of spins in Fe ions and redox behavior based on the Fe^{II}/Fe^{III} couple. Therefore, preparation of new tetrairon clusters must be important for developing new materials of functional significance.

Many oxo- and/or hydroxo-bridged tetrairon(III) complexes have been prepared and crystallographically characterized because they are easily obtained under basic conditions.[6] However, attempts to control the redox properties of oxo-bridged tetrairon clusters by changing the co-ligand and to prepare chemically or electrochemically their mixed-valence state are scarcely reported, whereas there are many reports about redox properties and mixed-valence states of oxo-bridged di- and tri-iron complexes.[6,7]

Previously, we have reported synthesis, structure, and magnetic property of a di-μ-oxo-bis[di-μ-phenolatodiiron(III)] complex, $[\{Fe_2(L)(OAc)\}_2(\mu\text{-}O)_2](PF_6)_2$ (**1**), where H_2L is the dinucleating compartmental ligand derived from the cyclic [2 + 2] condensation of 2,6-diformyl-4-methylphenol and 1,3-diaminopropane (Scheme 1) and acetate is a terminal co-ligand.[8] In this work, a series of tetranuclear di-μ-oxo-bis[di-μ-phenolatodiiron(III)] complexes with the general formula $[\{Fe_2(L)(L')\}_2(\mu\text{-}O)_2](PF_6)_2$ (**2**–**11**), where $(L')^-$ is a monochloroacetate (mca^-) for **2**, dichloroacetate (dca^-) for **3**, trifluoroacetate (tfa^-) for **4**, pentafluoropropionate ($pfpa^-$) for **5**, benzoate (BzO^-) for **6**, *p*-nitrobenzoate ($p\text{-}nba^-$) for **7**, pentafluorobenzoate ($pfba^-$) for **8**, diethylphosphate (dep^-) for **9**, diphenylphosphate (dpp^-) for **10**, and diethyldithiophosphate ($detp^-$) for **11**, were prepared. These complexes were crystallographically and magnetochemically characterized, and then electrochemical properties were studied. Furthermore, the oxo-bridged tetranuclear mixed-valence $Fe_4^{II,II,III,III}$ complexes were produced in situ by electrochemical reduction.

Results and Discussion

Preparation and Characterization. A compartmental ligand, L^{2-}, has been used to afford di(μ-phenolate) dinuclear complexes with an essentially planar structure.[9] Dimerization of a dinuclear complex with L^{2-} in the face-to-face mode, using an appropriate bridging ligand, may produce tetranuclear metal complexes. Such dimerization of a dinuclear unit with oxo bridge is often used for the synthesis of μ-oxo tetrairon(III) complexes.[10–12] The synthesis of **1** has been carried out by reacting iron(III) acetate, 2,6-diformyl-4-methylphenol,

† Present address: Tokyo University of Science, 1-3 Kagurazaka, Shinjuku-ku, Tokyo 162-8601

†† Present address: Department of Synthetic Chemistry and Biological Chemistry, Graduate School of Engineering, Kyoto University, Katsura, Nishikyo-ku, Kyoto 615-8510

Published on the web August 10, 2007; doi:10.1246/bcsj.80.1534

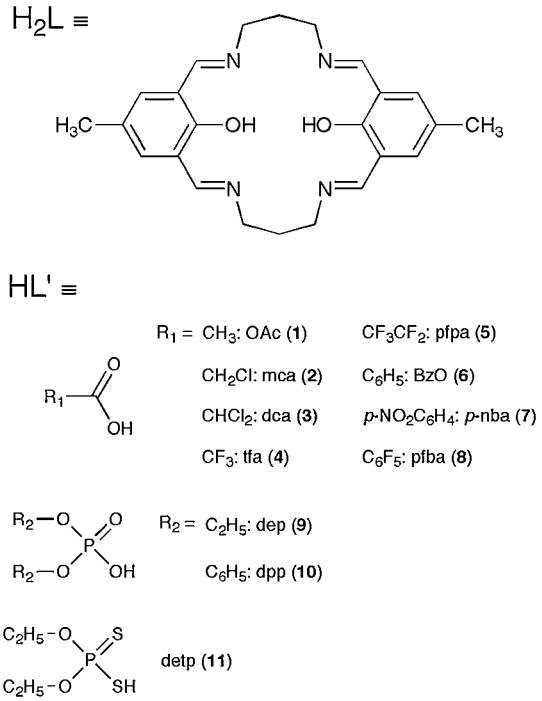

Scheme 1. A phenol-based macrocyclic ligand (H_2L) and the end-cap ligands (HL′).

and 1,3-diaminopropane in a 1:1:1 molar ratio in ethanol (Method A).[8] In this work, other synthetic methods (Method B and C) of **1** were examined in detail, because of preparation of analogues bearing other end-cap ligands. In Method B, the sodium salt of the macrocyclic ligand, Na_2L, was reacted with $Fe(OAc)_2(OH)$ in ethanol. In Method C, Na_2L was reacted with iron(III) chloride and sodium acetate in a 1:2:6 molar ratio in methanol. In all the synthetic methods, complex **1** precipitated on adding NH_4PF_6 to the respective reaction solution. Complexes **2**–**11** were prepared by Method C using a sodium carboxylate for **2**–**8**, sodium diethylphosphate for **9**, sodium diphenylphosphate for **10**, and sodium diethyldithiophosphate for **11**. We also confirmed that complex **1** could be converted into **6** by treatment with excess sodium benzoate (Method D). However, this method was not used for the synthesis of other complexes.

The ν(C=N) vibration of L^{2-} for **1**–**11** was observed around 1640 cm^{-1}. In the complexes with carboxylate analogues as the end-cap ligand, the ν_{as}(COO) and ν_s(COO) vibrations were found at 1563–1642 and 1435–1440 cm^{-1}, respectively. The ν_{as}(Fe–O_{oxo}–Fe) band is generally observed in the range from 850 to 870 cm^{-1},[6] but that of **1**–**11** was concealed by strong ν(PF) vibration of hexafluorophosphate ion at 843–846 cm^{-1}.

The UV–vis spectra of **1**–**11** in acetonitrile showed an intense absorption band at ≈350 nm ($\varepsilon \approx 22000\ M^{-1}\ cm^{-1}$) together with a discernible shoulder at ≈400 nm. The former was assigned to the π–π^* transition band associated with the azomethine group of L^{2-}, and the latter was assigned to the charge-transfer band from oxo to Fe^{III}.[6,13] No absorption band was recognized in the visible region in accord with the high-spin d^5 electronic configuration of Fe^{III}. An electronic spectrum of **4** is shown in Fig. 1.

Crystal Structures. Crystal structures of **4**, **7**, and **9** were

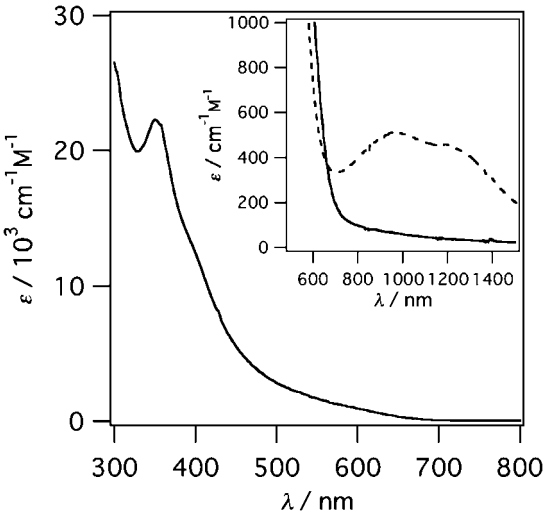

Fig. 1. UV–vis spectra of **4** (solid line) and its mixed-valence $Fe_4^{II,II,III,III}$ species produced by electrochemical reduction (dashed line in inset) in acetonitrile.

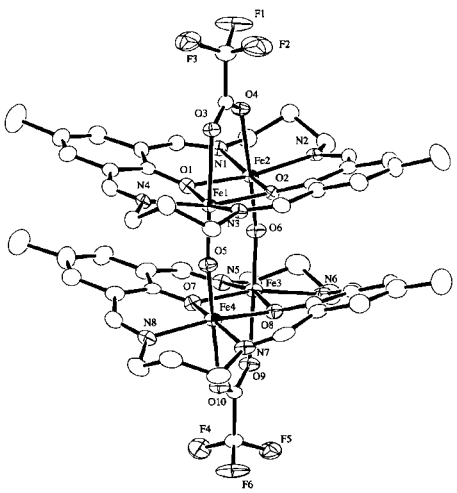

Fig. 2. A structure of cationic part of **4**.

determined. The structure of cationic part of **4** is shown in Fig. 2 together with the atom numbering. Average bond distances, angles, and interatomic separations for **4**, **7**, and **9** are summarized in Table 1.

The cationic parts of **4**, **7**, and **9** consisted of two dinuclear {Fe_2(L)(L′)} units and two oxo ligands, showing the same tetranuclear Fe_4O_6 core of "face-to-face" type as **1**.[8] Two Fe^{III} ions in a dinuclear unit were bridged by two phenolate of L^{2-} and carboxylate analogues or diethylphosphate as end-cap ligand in the *syn*,*syn*-mode. Each Fe^{III} ion in a dinuclear unit were connected to each Fe^{III} ion in another dinuclear unit by an oxo ligand. The coordination geometries of the Fe centers were pseudo-octahedral with the N_2O_2-donor atoms of L^{2-} at the equatorial position and with two O-donor atoms of an end-cap ligand and an oxo ligand at the axial site. The four Fe^{III} ions of **4** and **9** were crystallographically inequivalent. The cationic part of **9** had a mirror plane, which consisted of four iron atoms, two oxide ions, four oxygen atoms of dep^- and two phosphorus atoms of dep^-. Asymmetric unit of **7** con-

Table 1. Average Bond Distances (Å), Bond Angles (°), and Interatomic Separations (Å) for **4**, **7A**, **7B**, and **9**

	4	**7A**	**7B**	**9**
Fe–$O_{phenoxo}$	2.041	2.065	2.063	2.047
Fe–N	2.073	2.092	2.094	2.082
Fe–$O_{end\text{-}cap}$	2.242	2.177	2.176	2.163
Fe–O_{oxo}	1.778	1.796	1.794	1.786
Fe–O_{oxo}–Fe	163.6	153.1(2)[c]	153.4	162.7
Fe–$O_{phenoxo}$–Fe	97.6	97.2	97.4	97.9
Fe···Fe[a]	3.071	3.097(1)[c]	3.100	3.088
Fe···Fe[b]	3.520	3.492(1)[c]	3.491	3.531

a) In a dinuclear {Fe_2(L)(L′)} unit. b) Between dinuclear {Fe_2(L)(L′)} units. c) Unaveraged value is described in order to have the only one angle and interatomic separation.

sisted of two independent molecules (**7A** and **7B**). **7A** and **7B** formed similar bis-μ-oxo tetranuclear structure and showed no significant difference in the average bond distances and angles around the Fe centers. **7A** had a C_2 axis through a center of O7 and O7*, whereas **7B** had no symmetric operations.

Some geometrical characteristics about the tetranuclear cores of **1**,[8] **4**, **7A**, **7B**, and **9** were found. Four Fe^{III} and two O(oxo) atoms of **1** and **9** were coplaner. Those of **4** were nearly coplaner, and the dihedral angle between two least-squear planes, {Fe1, Fe2, O5, O6} and {Fe3, Fe4, O5, O6}, of **4** was 179.6°. The two {Fe_2(L)(*p*-nba)} units of **7A** and **7B** were obviously bent with respect to the O(oxo)···O(oxo) edge compared to **1**, **4**, and **9**. In **7A**, one least-squares plane formed by Fe1, Fe2, O7, and O7* and the other least-squares plane formed by Fe1*, Fe2*, O7, and O7* had a dihedral angle of 164.2°. In **7B**, the dihedral angle between two least-squares planes formed by Fe3, Fe4, O14, and O15 and by Fe5, Fe6, O14, and O15 was 163.8°. The apparent bend for two least-squares planes of **7A** and **7B** compared to **1**, **4**, and **9** did not influence the magnetochemical and electrochemical property, as discussed below. The average Fe–N and Fe–O bond distances and the Fe–O(phenoxo)–Fe angles on the equatorial plane of the dinuclear {Fe_2(L)(L′)} core for **1**, **4**, **7A**, **7B**, and **9** were slightly affected by changing the end-cap ligand. It must be noted that the Fe–O(tfa) bond of **4** (average 2.242 Å) was considerably elongated relative to the Fe–O(L′) bonds of **1**, **7A**, **7B**, and **9** (2.121–2.177 Å). The elongation of the Fe–O(L′) distance of **4** compared to **1**, **7A**, **7B**, and **9** is due to the decreased donor ability of the trifluoroacetate ligand. On the other hand, Fe–O(oxo) bond distances of **1**, **4**, **7A**, **7B**, and **9** were typical of Fe^{III}–O(oxo)–Fe^{III} linkages (1.755–1.820 Å),[6] and the Fe–O(oxo) bond of **4** (1.778 Å) was shorter than the bond distances of **1**, **7A**, **7B**, and **9** (1.784–1.796 Å).

Magnetic Properties. Magnetic susceptibilities of **2**–**11** were measured in the temperature range of 2–300 K. The temperature-dependence of the magnetic susceptibility and the magnetic moment for **4** is shown in Fig. 3. Complex **4** had a subnormal magnetic moment (1.89 μ_B per Fe) at 300 K, and the moment decreased with decreasing temperature to reach 0.23 μ_B at 2 K. It was found that a strong antiferromagnetic interaction operates within the molecule. Magnetic analysis was carried out by using the following magnetic susceptibility expression, which is based on the molecular field approximation:[14]

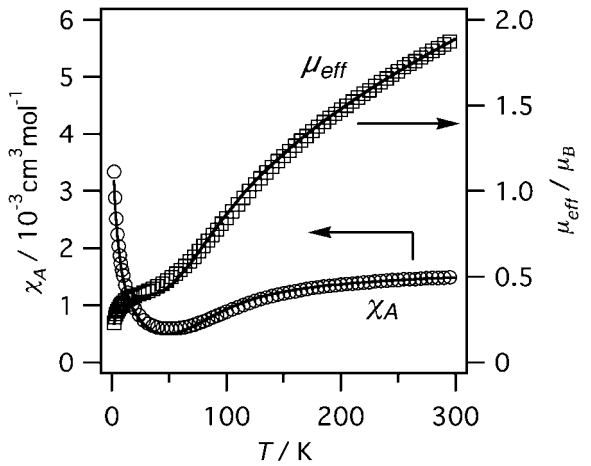

Fig. 3. Temperature-dependence of χ_A and μ_{eff} for **4**.

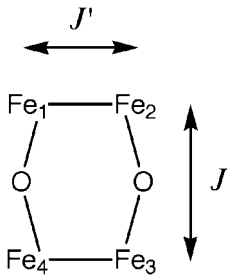

Scheme 2. Magnetic interactions within a dinuclear unit (J') and between dinuclear units (J).

$$\chi_A = (1-\rho)\frac{Ng^2\beta^2}{kT-2J'F}F + \rho\frac{35Ng^2\beta^2}{12k(T-\theta)}, \quad (1)$$

where $F = \{x + 5x^3 + 14x^6 + 30x^{10} + 55x^{15}\}/\{1 + 3x + 5x^3 + 7x^6 + 9x^{10} + 11x^{15}\}$ with $x = \exp(2J/kT)$. J' is the exchange integral between the Fe^{III} ions in a dinuclear {Fe_2(L)(L′)} unit, and J is the exchange integral between two Fe^{III} centers bridged by oxo ligand (Scheme 2). In this expression, ρ is the fraction of paramagnetic impurities, θ is the correction term for magnetic interaction of the paramagnetic impurities, and the remaining symbols have their usual physical meanings. The temperature-dependence of the magnetic susceptibility of **4** was reproduced by using of Eq. 1 with $J = -100\,cm^{-1}$, $J' = -10\,cm^{-1}$, $\rho = 0.005$, $\theta = -0.9$ K, and $g = 2.00$. Obtained J and J' values are close to those of **1** ($J = -101\,cm^{-1}$ and $J' = -11\,cm^{-1}$).[8] In addition, the large negative J values are typical of μ-oxodiiron(III) complexes, and the moderate negative J' values are also common for di(μ-phenolate)diiron(III) complexes.[6,15,16] The other complexes also showed similar magnetic behavior, and the magnetic interactions were explained by the Eq. 1. The best-fit parameters of **1**–**11** are summarized in Table 2. Obtained J and J' values for **2** and **3** and **5**–**11** were in the range of −94–−120 and −5–−12 cm^{-1}, respectively, and close to those of **1** and **4**.

Electrochemical Properties and Mixed-Valence Complexes. Electrochemical properties of **1**–**11** were studied by means of cyclic voltammetry in acetonitrile. The cyclic voltammogram of **4** is shown in Fig. 4. It showed a quasi-reversible couple at −313 mV (vs. Ag/Ag^+) and a pseudo-reversible

wave near −966 mV. The first redox couple was a two-electron-transfer process based on coulometric studies, thus, this wave was attributed to the $Fe_4^{III,III,III,III}/Fe_4^{II,II,III,III}$ process. The formation of the mixed-valence species was evidenced by visible and near-IR spectroscopy as discussed below. The second wave was also two-electron-transfer process and assigned to the $Fe_4^{II,II,III,III}/Fe_4^{II,II,II,II}$ process. The other complexes, except for **1** and **6**, had two waves from −332 to −574 and from −954 to −1080 mV. In the case of **1** and **6**, an irreversible wave was observed near −600 mV. These waves became quasi-reversible in the measurements in the presence of a large excess (ca. 100 times to complex) of sodium acetate for **1** and sodium benzoate for **6**, and the $E_{1/2}$ values for **1** and **6** were −567 and −537 mV, respectively. This fact implies that the end-cap ligands of **1** and **6** dissociate in solution when $Fe_4^{II,II,III,III}$ species is electrochemically prepared.

Table 2. Effective Magnetic Moments at 300 K and Best-Fit Parameters for **1**–**11**[a)]

	$\mu_{eff}(300\,K)/\mu_B$	J/cm^{-1}	J'/cm^{-1}	ρ	θ/K
1[8]	1.91	−101	−11	0.009	−1.5
2	1.84	−105	−11	0.005	−0.8
3	1.84	−103	−5	0.003	−0.9
4	1.89	−100	−10	0.005	−0.9
5	1.73	−113	−10	0.001	−2.0
6	1.68	−120	−12	0.009	−0.9
7	1.87	−103	−7	0.006	−0.8
8	1.89	−105	−4	0.011	−0.8
9	1.96	−94	−10	0.007	−1.2
10	1.74	−112	−10	0.002	−2.5
11	1.99	−102	−7	0.017	−1.9

a) The g values for **1**–**11** are fixed at 2.00.

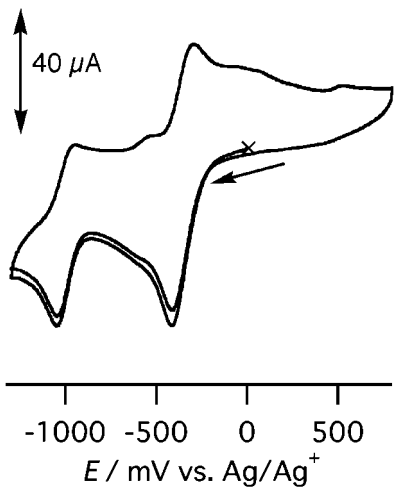

Fig. 4. Cyclic voltammogram of **4** (1 mM) in acetonitrile. TBAH (0.1 M) as supporting electrode, a glassy carbon as working electrode, a platimum wire as counter electrode, Ag/Ag^+ as reference electrode, and scan rate 100 mV s^{-1}.

The electrochemical data for **1**–**11** are summarized in Table 3. A $Fe_4^{III,III,III,III}/Fe_4^{II,II,III,III}$ redox potential depended on the nature of the end-cap ligand and shifted positive with a decrease in the pK_a value of the corresponding acid of end-cap ligand HL′ (Fig. 5).[17] Thus, the mixed-valence $Fe_4^{II,II,III,III}$ state is more stable when the donating ability of the end-cap ligand is smaller.

The mixed-valence $Fe_4^{II,II,III,III}$ species of **2**–**5** and **7**–**11**

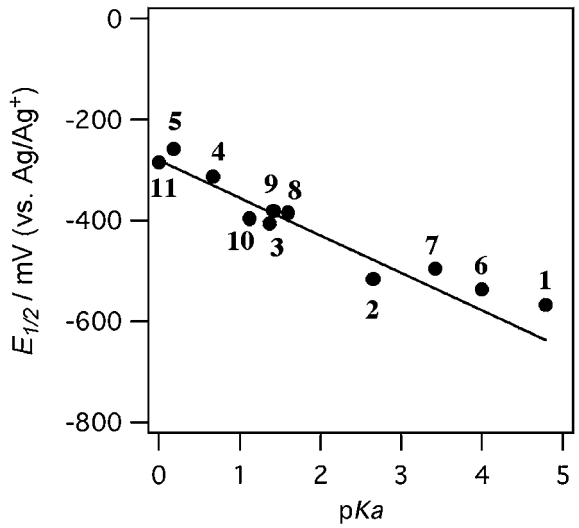

Fig. 5. Correlation between the $E_{1/2}$ of $Fe_4^{III,III,III,III}/Fe_4^{II,II,III,III}$ and pK_a value of HL′. The $E_{1/2}$ values of **1** and **6** are in the presence of excess amount of sodium acetate and benzoate, respectively.

Table 3. Electrochemical Data for **1**–**11** and Observed IT Band for Their $Fe_4^{II,II,III,III}$ Species in Acetonitrile, and pK_a Values of HL′

	$E_{cp}(1)$/mV	$E_{ap}(1)$/mV	$E_{1/2}(1)$[a)]/mV	$\Delta E(1)$[a)]/mV	$E_{cp}(2)$[b)]/mV	pK_a of HL′[d)]	IT band/nm (ε: $cm^{-1}\,M^{-1}$)
1[c)]	−620	—	—	—	−1110	4.79	
2	−574	−464	−516	110	−1080	2.65	938 (522), 1230 (433)
3	−470	−341	−406	129	−1050	1.37	918 (534), 1236 (415)
4	−376	−246	−313	130	−966	0.67	950 (515), 1230 (445)
5	−332	−184	−258	148	−1000	0.18	924 (522), 1236 (398)
6[c)]	−597	—	—	—	−1080	4.00	
7	−557	−440	−495	117	−1040	3.42	1020 (543)
8	−440	−327	−384	113	−1040	1.60	922 (376), 1226 (287)
9	−443	−313	−380	130	−1040	1.42	1006 (253), 1410 (203)
10	−447	−345	−396	102	−954	1.12	936 (340), 1250 (257)
11	−349	−221	−285	128	−1010	0	944 (383), 1244 (343)

a) $Fe_4^{III,III,III,III}/Fe_4^{II,II,III,III}$. b) $Fe_4^{II,II,III,III}/Fe_4^{II,II,II,II}$. c) In the absence of excess amount of sodium salt of $(L')^-$. d) Ref. 17.

were prepared by using electrolysis at −750 mV (vs. Ag/Ag^+) in acetonitrile. The spectrum of the mixed-valence complex of **4** is included in Fig. 1, and the numerical data of **2–5** and **7–11** are summarized in Table 3. These mixed-valence species showed characteristic absorption band in the range of 900–1500 nm (ε: 200–530 $cm^{-1}\,M^{-1}$ per molecule), whereas there was no absorption band in this range for the parent $Fe_4{}^{III,III,III,III}$ complexes and the electrochemically prepared $Fe_4{}^{II,II,II,II}$ species at −1500 mV (vs. Ag/Ag^+). The molar extinction coefficient of the present mixed-valence species in the near-IR region was relatively large compared to that of the ligand field band of an Fe^{II} complex (2–20 $cm^{-1}\,M^{-1}$ per Fe^{II}).[18] In addition, many mixed-valence diiron complexes have been reported to exhibit broad absorption band in the near-IR region.[19] Therefore, two relatively intense absorption bands for the present mixed-valence $Fe_4{}^{II,II,III,III}$ species in the near-IR area probably originate from the intervalence transition (IT) from Fe^{II} to Fe^{III}. Two characteristic IT bands were observed for the mixed-valence $Fe_4{}^{II,II,III,III}$ species of **2–5** and **8–11** similar to a dinuclear $Fe_2{}^{II,III}$ complex, $[Fe_2(HXTA)(OAc)_2]^{2-}$ (HXTA = *N*,*N*′-(2-hydroxy-5-methyl-1,3-xylylene)bis[*N*-(carboxymethyl)-glycine]).[19a] The separation of two IT bands of those species was at most 2900 cm^{-1} and too small to be assigned to the energy difference between t_{2g} and e_g orbitals in the O_h symmetry (i.e. 10 *Dq*). The geometry around the Fe^{III} center was approximated to be C_{4v}, since each iron(III) had a long Fe–O(end-cap) bond and a short Fe–O(oxo) bond relative to the equatorial bonds. The t_{2g} orbitals in O_h symmetry split into e and b_2 orbitals under C_{4v} symmetry, and the energy difference between the two IT bands seems to be comparable with the separation of the split e and b_2 orbitals. Therefore, we assigned the two IT bands on the electron transfer from the lowest t_{2g} orbital of Fe^{II} to the split e and b_2 orbitals of Fe^{III}. A mixed-valence species of **7** showed one IT band at 1020 nm (ε: 543 $cm^{-1}\,M^{-1}$), probably because of the overlap of two bands.

μ-Oxo-diiron(II, III) complexes generally show an IT band around 600 nm, whereas di(μ-carboxylate)-μ-phenolatodiiron(II, III) complexes show the IT band around 800–1200 nm.[20,21] In addition, electron-transfer rate is depended on the separation between Fe^{III} and Fe^{II} ions.[22] From crystallographic analysis, the separations of Fe^{III} ions within a dinuclear units and between dinuclear units for **4** were 3.071 and 3.520 Å, respectively. Therefore, the IT bands of the present complexes probably result from electron transfer within the dinuclear $\{Fe^{II}Fe^{III}(L)(L')\}$ unit.

Conclusion

A series of tetrairon(III) complexes, $[\{Fe_4(L)(L')\}_2(\mu\text{-}O)_2](PF_6)_2$ where $(L')^-$ is a carboxylate, phosphate, and dithiophosphate, were prepared, and the crystal structures of **4**, **7**, and **9** showed a di-μ-oxo-bis[di-μ-phenolatodiiron(III)] tetranuclear core similar to **1**. It is suggested that other complexes also have same tetranuclear structures. It is notable that the redox potentials of the present complexes shifted positive with a decrease in the pK_a value of HL′, whereas the magnetic properties were scarcely influenced by the end-cap ligand. Electrochemically prepared $Fe_4{}^{II,II,III,III}$ species showed an IT band in the range of 900–1500 nm. It is suggested that the electron transfer between Fe^{III} and Fe^{II} center mainly occurs in a dinuclear unit, because of the short metal···metal separation in a dinuclear unit compared to that between oxo-bridged two Fe centers.

Experimental

Physical Measurements. Elemental analyses of C, H, and N were obtained at the Elemental Analysis Service Center of Kyushu University. Metal analyses were made on a Shimadzu AA-660 atomic absorption/flame emission spectrometer. Infrared spectra were recorded on a Perkin-Elmer BX FT-IR system as KBr disks. Electronic absorption spectra were recorded in acetonitrile on a Shimadzu UV-3100PC spectrophotometer. Molar conductances were measured in acetonitorile using a DKK AOL-10 Conductivity Meter at room temperature. Magnetic susceptibilities of powdered samples were measured on a Quantum Design MPMS XL SQUID susceptometer in the temperature range of 2–300 K. Diamagnetic corrections were made using Pascal's constants. Cyclic voltammograms (CV) were recorded on a BAS CV-50W electrochemical analyzer in a degassed acetonitrile solution containing 0.1 M tetra(*n*-butyl)ammonium hexafluorophosphate (TBAH) as the supporting electrolyte. A three-electrode cell equipped with a glassy carbon as the working electrode, a platinum wire as the counter electrode, and an Ag/Ag^+ electrode as the reference electrode was used. Controlled-potential electrolyses were carried on the same instrument using a platinum-mesh as the working electrode.

Materials. 2,6-Diformyl-4-methylphenol and the dinucleating macrocyclic ligand (Na_2L) were prepared by using the literature methods.[23,24] Sodium *p*-nitrobenzoate, sodium pentafluorobenzoate, sodium diethylphosphate, sodium diphenylphosphate, sodium pentafluoropropionate, and sodium diethyldithiophosphate were prepared by the reaction of the respective acid with NaOH in methanol. Sodium acetate, sodium monochloroacetate, sodium dichloroacetate, and sodium trifluoroacetate were obtained from a commercial source.

Preparation of $[\{Fe_2(L)(AcO)\}_2(\mu\text{-}O)_2](PF_6)_2$ (1). Method A:[8] An ethanol solution of 1,3-diaminopropane (0.45 g, 6.09 mmol) was dropwise added to an ethanol solution of 2,6-diformyl-4-methylphenol (1.00 g, 6.09 mmol) and iron(III) acetate (1.42 g, 6.09 mmol), and the mixture was stirred at ambient temperature for 2 h. NH_4PF_6 (0.99 g, 6.09 mmol) was added to the reaction solution, and the mixture was stirred for 30 min to give a dark-brown precipitate. It was dissolved in acetonitrile, and the solution was diffused with diethyl ether to form reddish-brown crystals. Yield: 0.85 g (38%). Anal. Calcd for $C_{52}H_{58}N_8Fe_4F_{12}O_{10}P_2$: C, 42.53; H, 3.98; N, 7.63%. Found: C, 42.62; H, 4.03; N, 7.67%. Selected IR (ν/cm^{-1}): 1638, 1563, 1409, 843. μ_{eff} per Fe: 1.84 μ_B at 300 K. UV–vis (λ_{max}/nm ($\varepsilon/10^3\,cm^{-1}\,M^{-1}$)): 354 (22.0), 390 (sh) in acetonitrile. Molar conductance (Λ_M/$S\,cm^2\,mol^{-1}$): 291 in acetonitrile.

Method B: To a suspension of Na_2L (0.3 g, 0.67 mmol) and $Fe(AcO)_2(OH)$ (0.26 g, 1.34 mmol) in hot ethanol (20 mL) was added an ethanolic solution of triethylamine (0.14 g, 1.34 mmol), and the mixture was stirred for 1 h. NH_4PF_6 (0.44 g, 2.68 mmol) was added to the reaction solution, and the mixture was stirred at room temperature for 5 h to give a brown precipitate. It was dissolved in acetonitrile, and the solution was diffused with diethyl ether to obtain reddish-brown microcrystals. Yield: 0.12 g (24%).

Method C: To a suspension of Na_2L (0.3 g, 0.67 mmol) and $FeCl_3$ (0.22 g, 1.34 mmol) in hot methanol (20 mL) were added sodium acetate (0.58 g, 4.01 mmol) and a methanolic solution of triethylamine (0.14 g, 1.34 mmol). The mixture was refluxed for

Table 4. Crystallographic Data for **4**, **7**, and **9**

	4	**7**	**9**
Formula	$C_{87}H_{77}N_{13}O_{10}Fe_4F_{18}P_2$	$C_{62}H_{60}N_{10}O_{14}Fe_4P_2F_{12}$	$C_{58}H_{75}N_9O_{14}Fe_4F_{12}P_4$
Formula weight	2091.95	1682.53	1697.52
Temperature/°C	−90.0	25.0	25.0
Crystal system	monoclinic	monoclinic	orthorhombic
Space group	$P2_1/a$	$C2/c$	*Pnma*
a/Å	21.615(5)	36.71(1)	24.152(1)
b/Å	18.268(4)	28.890(8)	21.0974(9)
c/Å	24.275(6)	23.374(7)	13.8449(6)
α/°	90	90	90
β/°	109.814(2)	107.496(3)	90
γ/°	90	90	90
V/Å^3	9018(4)	23643(12)	7054(1)
Z value	4	12	4
D_{calcd}/g cm^{-3}	1.541	1.418	1.600
μ(Mo Kα)/cm^{-1}	7.68	8.52	9.95
No. of Ref. Meased.	70008	96707	55165
No. of Observations	20314 (all data)	26750 (all data)	8179 (all data)
	10735 ($I > 2\sigma$)	16390 ($I > 2\sigma$)	6007 ($I > 2\sigma$)
R (Rw)[a)] (all data)	0.141 (0.228)	0.153 (0.256)	0.120 (0.219)
R_1[b)] ($I > 2\sigma$)	0.093	0.095	0.068
Goodness of fit	1.24	1.54	1.38

a) $R = \Sigma[|F_o|^2 - |F_c|^2]/\Sigma|F_o|^2$; $Rw = [(\Sigma w(|F_o|^2 - |F_c|^2)^2/\Sigma w|F_o|^2)^2]^{1/2}$; $w = 1/\sigma^2(F_o)^2$.
b) $R_1 = \Sigma[|F_o| - |F_c|]/\Sigma|F_o|$.

1 h and filtered. NH_4PF_6 (0.44 g, 2.68 mmol) was added to the filtrate, and then the mixture was stirred at room temperature for 8 h to give a brown precipitate. It was dissolved in acetonitrile, and the solution was diffused with diethyl ether to obtain reddish-brown microcrystals. Yield: 0.15 g (30%).

Preparation of [{Fe$_2$(L)(L′)}$_2$(μ-O)$_2$](PF$_6$)$_2$ (2–11). These complexes were obtained by the Method C for the synthesis of **1**, using the respective sodium salt of HL′ instead of sodium acetate.

[{Fe$_2$(L)(mca)}$_2$(μ-O)$_2$](PF$_6$)$_2$·3H$_2$O (2): Reddish-brown crystals. Yield: 67%. Anal. Calcd for $C_{52}H_{62}N_8Fe_4Cl_2F_{12}O_{13}P_2$: C, 39.25; H, 3.93; N, 7.04; Fe, 14.04%. Found: C, 39.35; H, 4.07; N, 7.06; Fe, 13.53%. Selected IR [ν/cm^{-1}]: 1642, 1582, 1409, 846, 807. μ_{eff} per Fe: 1.84 μ_B at 300 K. UV–vis (λ_{max}/nm (ε/10^3 cm^{-1} M^{-1})): 358 (21.6), 400 (sh) in acetonitrile. Molar conductance (Λ_M/S cm^2 mol^{-1}): 270 in acetonitrile.

[{Fe$_2$(L)(dca)}$_2$(μ-O)$_2$](PF$_6$)$_2$·2H$_2$O (3): Reddish-brown crystals. Yield: 68%. Anal. Calcd for $C_{52}H_{58}N_8Fe_4Cl_4F_{12}O_{12}P_2$: C, 38.03; H, 3.56; N, 6.82%. Found: C, 37.82; H, 3.41; N, 6.74%. Selected IR [ν/cm^{-1}]: 1642, 1607, 1374, 845, 807. μ_{eff} per Fe: 1.84 μ_B at 300 K. UV–vis (λ_{max}/nm (ε/10^3 cm^{-1} M^{-1})): 352 (22.1), 390 (sh) in acetonitrile. Molar conductance (Λ_M/S cm^2 mol^{-1}): 281 in acetonitrile.

[{Fe$_2$(L)(tfa)}$_2$(μ-O)$_2$](PF$_6$)$_2$·3PhCN·2H$_2$O (4): Crystallized from benzonitrile as reddish-brown crystals. Yield: 62%. Anal. Calcd for $C_{73}H_{71}N_{11}Fe_4F_{18}O_{12}P_2$: C, 45.63; H, 3.72; N, 8.02; Fe, 11.62%. Found: C, 45.24; H, 3.50; N, 7.97; Fe, 11.57%. Selected IR [ν/cm^{-1}]: 1642, 1562, 1439, 1318, 1199, 845. μ_{eff} per Fe: 1.84 μ_B (powder) at 300 K. UV–vis (λ_{max}/nm (ε/10^3 cm^{-1} M^{-1})): 350 (22.3), 380 (sh) in acetonitrile. Molar conductance (Λ_M/S cm^2 mol^{-1}): 282 in acetonitrile.

[{Fe$_2$(L)(pfpa)}$_2$(μ-O)$_2$](PF$_6$)$_2$ (5): Reddish-brown crystals. Yield: 73%. Anal. Calcd for $C_{54}H_{52}N_8Fe_4F_{22}O_{10}P_2$: C, 38.96; H, 3.13; N, 6.68%. Found: C, 38.96; H, 3.16; N, 6.70%. Selected IR [ν/cm^{-1}]: 1643, 1562, 1439, 1319, 845, 815. μ_{eff} per Fe: 1.73 μ_B at 300 K. UV–vis (λ_{max}/nm (ε/10^3 cm^{-1} M^{-1})): 352 (21.5), 380 (sh) in acetonitrile. Molar conductance (Λ_M/S cm^2 mol^{-1}): 279 in acetonitrile.

[{Fe$_2$(L)(BzO)}$_2$(μ-O)$_2$](PF$_6$)$_2$ (6): Reddish-brown crystals. Yield: 46%. Anal. Calcd for $C_{62}H_{62}N_8Fe_4F_{12}O_{10}P_2$: C, 46.76; H, 3.92; N, 7.04%. Found: C, 46.72; H, 4.12; N, 6.98%. Selected IR [ν/cm^{-1}]: 1641, 1563, 1388, 845, 807. μ_{eff} per Fe: 1.81 μ_B at 300 K. UV–vis (λ_{max}/nm (ε/10^3 cm^{-1} M^{-1})): 358 (24.0), 390 (sh) in acetonitrile. Molar conductance (Λ_M/S cm^2 mol^{-1}): 234 in acetonitrile.

The same complex was also obtained when **1** was treated with excess sodium benzoate in a methanol–acetonitrile mixture (Method D). Yield: 26%.

[{Fe$_2$(L)(*p*-nba)}$_2$(μ-O)$_2$](PF$_6$)$_2$ (7): Reddish-brown crystals. Yield: 70%. Anal. Calcd for $C_{62}H_{60}N_{10}Fe_4F_{12}O_{14}P_2$: C, 44.26; H, 3.59; N, 8.32; Fe, 13.28%. Found: C, 44.41; H, 3.64; N, 8.43; Fe, 12.47%. Selected IR [ν/cm^{-1}]: 1641, 1562, 1389, 844, 817. μ_{eff} per Fe: 1.87 μ_B at 300 K. UV–vis (λ_{max}/nm (ε/10^3 cm^{-1} M^{-1})): 354 (22.9), 400 (sh) in acetonitrile. Molar conductance (Λ_M/S cm^2 mol^{-1}): 277 in acetonitrile.

[{Fe$_2$(L)(pfba)}$_2$(μ-O)$_2$](PF$_6$)$_2$ (8): Reddish-brown crystals. Yield: 75%. Anal. Calcd for $C_{62}H_{52}N_8Fe_4F_{22}O_{10}P_2$: C, 42.01; H, 2.96; N, 6.32%. Found: C, 41.90; H, 3.06; N, 6.39%. Selected IR [ν/cm^{-1}]: 1642, 1593, 1376, 846, 810. μ_{eff} per Fe: 1.89 μ_B at 300 K. UV–vis (λ_{max}/nm (ε/10^3 cm^{-1} M^{-1})): 352 (21.5), 390 (sh) in acetonitrile. Molar conductance (Λ_M/S cm^2 mol^{-1}): 264 in acetonitrile.

[{Fe$_2$(L)(dep)}$_2$(μ-O)$_2$](PF$_6$)$_2$·MeCN (9): Reddish-brown crystals. Yield: 71%. Anal. Calcd for $C_{58}H_{75}N_9Fe_4F_{12}O_{14}P_4$: C, 41.04; H, 4.45; N, 7.43; Fe, 13.16%. Found: C, 40.96; H, 4.39; N, 7.41; Fe, 13.49%. Selected IR [ν/cm^{-1}]: 1642, 1561, 1437, 1319, 1075, 1060, 842. μ_{eff} per Fe: 1.96 μ_B at 300 K. UV–vis (λ_{max}/nm (ε/10^3 cm^{-1} M^{-1})): 354 (22.9), 400 (sh) in acetonitrile. Molar conductance (Λ_M/S cm^2 mol^{-1}): 299 in acetonitrile.

[{Fe_2(L)(dpp)}$_2$(μ-O)$_2$](PF_6)$_2$·H_2O (10): Reddish-brown crystals. Yield: 65%. Anal. Calcd for $C_{72}H_{74}N_8Fe_4F_{12}O_{15}P_4$: C, 46.33; H, 4.00; N, 6.00%. Found: C, 46.15; H, 3.94; N, 5.97%. Selected IR [ν/cm^{-1}]: 1639, 1561, 1318, 1201, 1084, 845. μ_{eff} per Fe: 1.74 μ_B at 300 K. UV–vis (λ_{max}/nm (ε/10^3 cm^{-1} M^{-1})): 356 (20.7), 400 (sh) in acetonitrile.

[{Fe_2(L)(detp)}$_2$(μ-O)$_2$](PF_6)$_2$·MeCN (11): Reddish-brown crystals. Yield: 47%. Anal. Calcd for $C_{58}H_{75}N_9Fe_4F_{12}O_{10}P_4S_4$: C, 39.54; H, 4.29; N, 7.16; Fe, 12.68%. Found: C, 39.78; H, 4.16; N, 7.10; Fe, 12.64%. Selected IR [ν/cm^{-1}]: 1640, 1563, 1438, 1316, 843, 816, 557. μ_{eff} per Fe: 1.99 μ_B at 300 K. UV–vis (λ_{max}/nm (ε/10^3 cm^{-1} M^{-1})): 354 (22.9), 400 (sh) in acetonitrile. Molar conductance (Λ_M/S cm^2 mol^{-1}): 263 in acetonitrile.

X-ray Crystallographic Analyses. A single crystals of **4**, **7**, and **9** were coated with epoxy resin. Crystallographic measurements of **4**, **7**, and **9** were made on a Rigaku/MSC Mercury CCD diffractometer with graphite monochromated Mo Kα (λ = 0.71070 Å) radiation. The data were collected at -90 ± 1 °C for **4** and at 25 ± 1 °C for **7** and **9**, to a maximum 2θ value of 55.0°. A total of 1240 oscillation images were collected. Data were collected and processed using the Crystalclear program (Rigaku). The linear absorption coefficients, μ, for Mo Kα radiation of **4**, **7**, and **9** were 7.68, 8.52, and 9.95 cm^{-1}, respectively. The data were corrected for Lorentz and polarization effects.

The structures of **4**, **7**, and **9** were solved by Patterson methods (DIRDIF94 PATTY),[25] direct methods (SIR-92),[26] and direct methods (SAPI 90),[27] respectively. All of the structures were expanded using Fourier techniques. The non-hydrogen atoms were refined anisotropically. Hydrogen atoms were included for structure analysis but not refined. The final cycle of full-matrix least-squares refinement was based on all reflections ($2\theta < 54.97$). Computations were carried out on a SGI O2 computer using teXsan crystallographic software package.[28]

Crystallographic data and details of the structure determinations for **4**, **7**, and **9** are summarized in Table 4. Crystallographic data have been deposited at the CCDC, 12, Union Road, Cambridge, CB2 1EZ, UK (http://www.ccdc.cam.ac.uk/conts/retrieving.html; Fax: +44 1223 336033; e-mail: deposit@ccdc.cam.ac.uk). Copies can be obtained on request, free of charge, by quoting the publication citation and the deposition numbers, CCDC-610451, -610452, and -610453 for compounds Nos. **4**, **7**, and **9**, respectively.

This work was supported by a Grant-in-Aid (No. 13640561) from the Ministry of Education, Culture, Sports, Science and Technology.

Supporting Information

Selected bond distances, bond angles, and interatomic separations of **4**, **7A**, **7B**, and **9** (Table S1), and the structures of cationic parts of **7A**, **7B**, and **9** (Figs. S1–S3). This material is available free of charge on the web at: http://www.csj.jp/journals/bcsj/.

References

1 a) L. Que, Jr., A. E. True, *Prog. Inorg. Chem.* **1990**, Vol. 38, p. 97. b) S. J. Lippard, *Angew. Chem., Int. Ed. Engl.* **1988**, *27*, 344.

2 a) D. Gatteschi, R. Sessoli, A. Cornia, *Chem. Commun.* **2000**, 725. b) A. L. Barra, A. Caneschi, A. Cornia, F. F. Biani, D. Gatteschi, C. Sangregorio, R. Sessoli, L. Sorace, *J. Am. Chem. Soc.* **1999**, *121*, 5302.

3 H. Oshio, N. Hoshino, T. Ito, *J. Am. Chem. Soc.* **2000**, *122*, 12602.

4 P. V. Rao, R. H. Holm, *Chem. Rev.* **2004**, *104*, 527.

5 H. Beinert, R. H. Holm, E. Münck, *Science* **1997**, *277*, 653.

6 a) D. M. Kurtz, Jr., *Chem. Rev.* **1990**, *90*, 585. b) J. B. Vincent, G. L. Olivier-Lilley, B. A. Averill, *Chem. Rev.* **1990**, *90*, 1447.

7 a) L. Keeney, M. J. Hynes, *Dalton Trans.* **2005**, 1524. b) A. M. Bond, R. J. H. Clark, D. G. Humphrey, P. Panayiotopoulos, B. W. Skelton, A. H. White, *J. Chem. Soc., Dalton Trans.* **1998**, 1845. c) P. Poganiuch, S. Liu, G. C. Papaefthymiou, S. J. Lippard, *J. Am. Chem. Soc.* **1991**, *113*, 4645.

8 Y. Miyasato, Y. Nogami, M. Ohba, H. Sakiyama, H. Ōkawa, *Bull. Chem. Soc. Jpn.* **2003**, *76*, 1009.

9 H. Ōkawa, H. Furutachi, D. E. Fenton, *Coord. Chem. Rev.* **1998**, *174*, 51.

10 a) B. P. Murch, P. D. Boyle, L. Que, Jr., *J. Am. Chem. Soc.* **1985**, *107*, 6728. b) B. P. Murch, F. C. Bradley, P. D. Boyle, V. Papaefthymiou, L. Que, Jr., *J. Am. Chem. Soc.* **1987**, *109*, 7993.

11 a) K. B. Jensen, C. J. McKenzie, O. Simonsen, H. Toftlund, A. Hazell, *Inorg. Chim. Acta* **1997**, *257*, 163. b) H. Toftlund, K. S. Murray, P. R. Zwack, L. F. Taylor, O. P. Anderson, *J. Chem. Soc., Chem. Commun.* **1986**, 191.

12 J. H. Satcher, Jr., M. M. Olmstead, M. W. Droege, S. R. Parkin, B. C. Noll, L. May, A. L. Balch, *Inorg. Chem.* **1998**, *37*, 6751.

13 a) S. K. Dutta, R. Werner, U. Flörke, S. Mohanta, K. K. Nanda, W. Haase, K. Nag, *Inorg. Chem.* **1996**, *35*, 2292. b) K. K. Nanda, S. K. Dutta, S. Baitalik, K. Venkatsubramanian, K. Nag, *J. Chem. Soc., Dalton Trans.* **1995**, 1239.

14 A. P. Gingsberg, *Inorg. Chim. Acta Rev.* **1971**, *5*, 45.

15 S. M. Gorun, S. J. Lippard, *Inorg. Chem.* **1991**, *30*, 1625.

16 B. Chiari, O. Piovesana, T. Tarantelli, P. F. Zanazzi, *Inorg. Chem.* **1983**, *22*, 2781.

17 The pK_a values of HL′ are calculated by using Advanced Chemistry Development (ACD/Labs) software (Ver. 8.14) for Solaris.

18 a) J. S. Loehr, T. M. Loehr, A. G. Mauk, H. B. Gray, *J. Am. Chem. Soc.* **1980**, *102*, 6992. b) M. Suzuki, S. Fujinami, T. Hibino, H. Hori, Y. Maeda, A. Uehara, M. Suzuki, *Inorg. Chim. Acta* **1998**, *283*, 124.

19 a) A. S. Borovik, B. P. Murch, L. Que, Jr., V. Papaefthymiou, E. Münck, *J. Am. Chem. Soc.* **1987**, *109*, 7190. b) S. K. Dutta, J. Ensling, R. Werner, U. Flörke, W. Haase, P. Gütlich, K. Nag, *Angew. Chem., Int. Ed. Engl.* **1997**, *36*, 152. c) A. S. Borovik, L. Que, Jr., *J. Am. Chem. Soc.* **1988**, *110*, 2345. d) M. S. Mashuta, R. J. Webb, J. K. McCusker, E. A. Schmitt, K. J. Oberhausen, J. F. Richardson, R. M. Buchanan, D. N. Hendrickson, *J. Am. Chem. Soc.* **1992**, *114*, 3815.

20 S. C. Payne, K. S. Hagen, *J. Am. Chem. Soc.* **2000**, *122*, 6399.

21 S. K. Dutta, J. Ensling, R. Werner, U. Flörke, W. Haase, P. Gütlich, K. Nag, *Angew. Chem., Int. Ed. Engl.* **1997**, *36*, 152.

22 a) A. S. Borovik, V. Papaefthymiou, L. F. Taylor, O. P. Anderson, L. Que, Jr., *J. Am. Chem. Soc.* **1989**, *111*, 6183. b) N. S. Hush, *Prog. Inorg. Chem.* **1967**, Vol. 8, p. 391.

23 L. F. Lindoy, G. V. Meehan, N. Svenstrup, *Synthesis* **1998**, 1029.

24 a) S. Gou, D. E. Fenton, *Inorg. Chim. Acta* **1994**, *223*, 169. b) H. Adams, N. A. Bailey, P. Bertland, O. R. Cecilia, D. E.

Fenton, S. Gou, *J. Chem. Soc., Dalton Trans.* **1995**, 275.

25 PATTY: P. T. Beurskens, G. Admiraal, G. Beurskens, W. P. Bosman, R. de Gelder, R. Israel, J. M. M. Smits, *The DIRDIF-94 Program System, Technical Report of the Crystallography Laboratory*, University of Nijmegen, The Netherlands, **1994**.

26 SIR-92: A. Altomare, G. Cascarano, C. Giacovazzo, A. Guagliardi, M. C. Burla, G. Polidori, M. Camalli, *J. Appl. Crystallogr.* **1994**, *27*, 435.

27 SAPI 90: F. Hai-Fu, *Structure Analysis Programs with Intelligent Control*, Rigaku Corporation, Tolyo, Japan, **1990**.

28 teXsan, ver. 1.11: *Single Crystal Structure Analysis Software*, Molecular Structure Corporation, The Woodlamds, TX, **1999**.